A RECEDING HORIZON CONTROLLER WITH A PARAMETER ESTIMATOR FOR NUCLEAR REACTOR POWER DISTRIBUTION

Man Gyun Na, Young Rok Sim and Sun Mi Lee
Chosun University, Nuclear Engineering Department
375 Seoseok-dong, Dong-gu, Gwangju 501-759, Korea
TEL: (82-62) 230-7168   FAX: (82-62) 232-7243
e-mail: magyna@chosun.ac.kr

ABSTRACT

A receding horizon control method is to solve on-line, at each time step, an optimization problem for a finite future and to implement the first optimal control input as the current control input. The receding horizon controller with a parameter estimator is applied to the axial power distribution control in a pressurized water reactor. It is a suitable control strategy for time-varying systems because the parameter estimator identifies a controller design model recursively at each time step and also, the receding horizon controller recalculates an optimal input at each time step by using newly measured signals. The reactor dynamics model used for computer simulations is a two-point xenon oscillation model based on the nonlinear xenon and iodine balance equations and a one-group, one-dimensional, neutron diffusion equation with nonlinear power reactivity feedback that adequately describes axial oscillations and treats the nonlinearities explicitly. The reactor core is axially divided into two regions, and each region is assumed to have single input and single output and be coupled with the other region. It is shown from numerical simulations that the proposed control algorithm exhibits very fast tracking responses due to the step and ramp changes of axial target shape and also works well in a time-varying parameter condition.

1. INTRODUCTION

Flux distribution unbalance which is usually caused by load-following operation in a reactor core induces xenon oscillation because the absorption cross-section of xenon is extremely large and its effects in a reactor are delayed by the iodine precursor. The fact that there is no direct way of measuring the xenon concentration often causes operators a great deal of difficulty in treating the xenon imbalance that is closely related to the axial power shape. Because the reactor power distribution control has been one of the most challenging control problems in the nuclear field, there have been extensive research activities in this area, especially using conventional optimal control methods [1-9].

The receding horizon control methodology has received a great deal of attention as a powerful tool for the control of industrial process systems [10-16]. The receding horizon control method is to solve on-line an optimization problem for a finite future at current time and to implement the first optimal control input as the current control input. This method has many advantages over the conventional infinite horizon control because it is possible to handle input and state (or output) constraints in a systematic manner during the design and implementation of the control. While some tracking controllers use only the current tracking command, the receding horizon control can achieve better tracking performance because future commands are considered in addition to the current tracking command. Therefore, in this work the receding horizon controller with a parameter estimator is applied to the axial power distribution control in a pressurized water reactor. Also, this applied controller is a suitable control strategy for time-varying systems because the parameter estimator identifies a controller design model recursively at each time step and also the receding horizon controller recalculates an optimal input at each time step by using newly measured signals.

In this paper, a two-point (lower and upper half) xenon oscillation model [17-19] is used to examine the proposed controller. The reactor core is modeled by being axially divided into two regions. Each region has one input and one output and is coupled with the other region. The controlled process has two inputs and two outputs and is described by a matrix polynomial model.

2. DESIGN OF A RECEDING HORIZON CONTROL SYSTEM

2.1. PROBLEM STATEMENT

The process to be controlled is described by the following controlled auto-regressive and integrated moving average (CARIMA) model, which is widely used as a mathematical model of control design methods:

$$\mathbf{A}(q^{-1})\mathbf{y}(t) = \mathbf{B}(q^{-1})\Delta\mathbf{u}(t-1) + \mathbf{C}(q^{-1})\xi(t) \ , \tag{1}$$

where $\mathbf{y} \in R^n$ is the output, $\mathbf{u} \in R^m$ is the control input change between time steps, $\xi \in R^m$ is a stochastic random noise vector sequence with zero mean value, q^{-1} is the backward shift operator, e.g., $q^{-1}\mathbf{y}(t) = \mathbf{y}(t-1)$, and Δ is defined as $\Delta = 1 - q^{-1}$. In Eq. (1), $\mathbf{A}(q^{-1})$ and $\mathbf{C}(q^{-1})$ are $n \times n$ monic matrix polynomials as a function of the backward shift operator q^{-1}, and $\mathbf{B}(q^{-1})$ is an $n \times m$ matrix polynomial. For example, the $n \times m$ matrix polynomial $\mathbf{B}(q^{-1})$ is expressed as follows:

$$\mathbf{B}(q^{-1}) = \mathbf{B}_0 + \mathbf{B}_1 q^{-1} + \mathbf{B}_2 q^{-2} + \ldots + \mathbf{B}_{nB} q^{-nB} \ , \tag{2}$$

where $\mathbf{B}_0, \mathbf{B}_1, \cdots, \mathbf{B}_{nB}$ are $n \times m$ real matrices and nB is the order of the matrix polynomial.

The basic idea of receding horizon control is to calculate a sequence of future control signals in such a way that it minimizes a multistage cost function defined over a finite prediction horizon. The associated performance index is the following quadratic function:

$$J = \frac{1}{2}\sum_{j=1}^{N}\left(\hat{\mathbf{y}}(t+j\,|\,t) - \mathbf{w}(t+j)\right)^T \mathbf{Q}\left(\mathbf{y}(t+j\,|\,t) - \mathbf{w}(t+j)\right) + \frac{1}{2}\sum_{j=1}^{M}\Delta\mathbf{u}(t+j-1)^T \mathbf{R}\Delta\mathbf{u}(t+j-1) \ , \tag{3}$$

subject to a constraint $\Delta\mathbf{u}(t+j-1) = \mathbf{0}$ for $j > M$ ($M < N$),

where positive definite matrices $\mathbf{Q}$ and $\mathbf{R}$ are symmetric matrices to weight particular components of $(\hat{\mathbf{y}} - \mathbf{w})$ and $\Delta\mathbf{u}$ at certain future time intervals, respectively, and $\mathbf{w}$ is a setpoint or reference sequence for the output vector. Also, $\hat{\mathbf{y}}(t+j\,|\,t)$ is an optimum j-step-ahead prediction of the system output based on data up to time t; that is, the expected value of the output vector at time t if the past input and output vectors and the future control sequence are known. Here, N is the minimum and maximum prediction horizons, respectively, and M is the control horizon. The prediction horizons represent the limits of the instants in which it is desired for the output to follow the reference sequence. To obtain control inputs, the predicted outputs have to be first calculated as a function of past values of inputs and outputs and of future control signals.

The receding horizon control method solves an optimization problem for a finite future at current time and implements the first optimal control input as the current control input. The procedure is then repeated at each subsequent instant. Figure 1 shows this basic concept of the receding horizon control method [12]. As it were, for any assumed set of current and future control moves, the future behavior of the process outputs can be predicted over a horizon N, and the M present and future control moves ($M \le N$) are computed to minimize a quadratic objective function. Although M control moves are calculated, only the first control move is implemented. At the next time step, new values of the measured output are obtained, the control horizon is shifted forward by one step, and the same calculations are repeated. The purpose of taking new measurements at each time step is to compensate for unmeasured disturbances and model inaccuracy, both of which cause the measured system output to be different from the one predicted by the model.

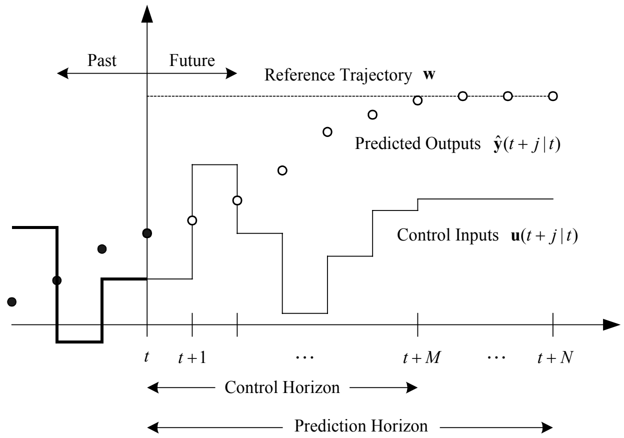

Figure 1. Basic concept of a receding horizon control method

2.2. DESIGN OF A RECEDING HORIZON CONTROLLER

The process output at time $t + j$ can be predicted from the measurements of the output and input up to time step t. The optimal prediction is derived by solving a Diophantine equation, whose solution can be found by an efficient recursive algorithm. In this derivation, the most usual case, when $\mathbf{C}(q^{-1}) = \mathbf{I}_{n\times n}$, will be considered. The j-step-ahead output prediction of the multivariable process is derived herein.

Multiplying Eq. (1) by $\mathbf{E}_j(q^{-1})$ from the left gives

$$\mathbf{y}(t+j) - \mathbf{E}_j(q^{-1})\xi(t+j) = \mathbf{F}_j(q^{-1})\mathbf{y}(t) + \mathbf{E}_j(q^{-1})\mathbf{B}(q^{-1})\Delta\mathbf{u}(t+j-1), \tag{4}$$

where $\mathbf{E}_j(q^{-1})$ and $\mathbf{F}_j(q^{-1})$ are the matrix polynomials satisfying

$$\mathbf{I}_{n\times n} = \mathbf{E}_j(q^{-1})\mathbf{A}(q^{-1}) + q^{-j}\mathbf{F}_j(q^{-1}), \tag{5}$$

$$\mathbf{E}_j(q^{-1}) = \mathbf{E}_{j,0} + \mathbf{E}_{j,1}q^{-1} + \cdots + \mathbf{E}_{j,j-1}q^{-(j-1)}, \tag{6}$$

$$\mathbf{F}_j(q^{-1}) = \mathbf{F}_{j,0} + \mathbf{F}_{j,1}q^{-1} + \mathbf{F}_{j,2}q^{-2} + \cdots + \mathbf{F}_{j,nA-1}q^{-nA+1}. \tag{7}$$

Equation (5) is called the Diophantine equation, and there exist unique matrix polynomials $\mathbf{E}_j(q^{-1})$ and $\mathbf{F}_j(q^{-1})$ of order $j-1$ and $nA-1$, respectively, such that $\mathbf{E}_{j,0} = \mathbf{I}_{n\times n}$. By taking the expectation operator and considering that $E\{\xi(t)\} = 0$, the optimal j-step-ahead prediction of $\hat{\mathbf{y}}(t+j\,|\,t)$ satisfies

$$\hat{\mathbf{y}}(t+j\,|\,t) = \mathbf{F}_j(q^{-1})\mathbf{y}(t) + \mathbf{G}_j(q^{-1})\Delta\mathbf{u}(t+j-1), \tag{8}$$

where $\hat{\mathbf{y}}(t+j\,|\,t) = E\{\mathbf{y}(t+j) - \mathbf{E}_j(q^{-1})\xi(t+j) | t\}$ which denotes an estimated value of the output at time step $t+j$ based on all the data up to time step t and $\mathbf{G}_j(q^{-1}) = \mathbf{E}_j(q^{-1})\mathbf{B}(q^{-1})$. The output prediction can easily be extended to the nonzero mean noise case by adding vector $\mathbf{E}_j(q^{-1})E\{\xi(t)\}$ to the output prediction $\hat{\mathbf{y}}(t+j\,|\,t)$.

By dividing the matrix polynomial $\mathbf{G}_j(q^{-1})$ into two terms like the following equation:

$$\mathbf{G}_j(q^{-1}) = \overline{\mathbf{G}}_j(q^{-1}) + q^{-j}\widetilde{\mathbf{G}}_j(q^{-1}) \quad \text{with} \quad \delta\left(\overline{\mathbf{G}}_j(q^{-1})\right) < j\,, \tag{9}$$

the prediction equation can now be written as

$$\hat{\mathbf{y}}(t+j\,|\,t) = \overline{\mathbf{G}}_j(q^{-1})\Delta\mathbf{u}(t+j-1) + \widetilde{\mathbf{G}}_j(q^{-1})\Delta\mathbf{u}(t-1) + \mathbf{F}_j(q^{-1})\mathbf{y}(t)\,, \tag{10}$$

where $\delta\left(\overline{\mathbf{G}}_j(q^{-1})\right)$ denotes the order of the polynomial $\overline{\mathbf{G}}_j(q^{-1})$.

The last two terms of the right side of Eq. (10) consist of past values of the process input and output variables and correspond to the free response of the process if the control signals are kept constant, while the first term consists of future values of the control input signal and can be interpreted as the forced response, that is, the response obtained when the initial conditions are zero $\mathbf{y}(t-j) = \mathbf{0}, \Delta\mathbf{u}(t-j-1) = \mathbf{0}$ for $j > 0$ [16]. Equation (10) can be rewritten as

$$\hat{\mathbf{y}}(t+j\,|\,t) = \overline{\mathbf{G}}_j(q^{-1})\Delta\mathbf{u}(t+j-1) + \mathbf{f}_j\,, \tag{11}$$

with $\mathbf{f}_j = \widetilde{\mathbf{G}}_j(q^{-1})\Delta\mathbf{u}(t-1) + \mathbf{F}_j(q^{-1})\mathbf{y}(t)$. Then a set of N j-ahead output predictions can be expressed as

$$\hat{\mathbf{y}} = \overline{\mathbf{G}}\Delta\mathbf{u} + \mathbf{f}\,, \tag{12}$$

where

$$\hat{\mathbf{y}} = \left[\hat{\mathbf{y}}(t+1\,|\,t)^T \quad \hat{\mathbf{y}}(t+2\,|\,t)^T \quad \cdots \quad \hat{\mathbf{y}}(t+j\,|\,t)^T \quad \cdots \quad \hat{\mathbf{y}}(t+N\,|\,t)^T\right]^T,$$

$$\Delta\mathbf{u} = \left[\Delta\mathbf{u}(t)^T \quad \Delta\mathbf{u}(t+1)^T \quad \cdots \quad \Delta\mathbf{u}(t+j)^T \quad \cdots \quad \Delta\mathbf{u}(t+N-1)^T\right]^T,$$

$$\mathbf{f} = \left[\mathbf{f}_1^T \quad \mathbf{f}_2^T \quad \cdots \quad \mathbf{f}_j^T \quad \cdots \quad \mathbf{f}_N^T\right]^T,$$

$$\overline{\mathbf{G}} = \begin{bmatrix} \mathbf{G}_0 & \mathbf{0} & \cdots & \mathbf{0} & \cdots & \mathbf{0} \\ \mathbf{G}_1 & \mathbf{G}_0 & \cdots & \mathbf{0} & \cdots & \mathbf{0} \\ \vdots & \vdots & \ddots & \vdots & \vdots & \vdots \\ \mathbf{G}_{j-1} & \mathbf{G}_{j-2} & \cdots & \mathbf{G}_0 & \cdots & \mathbf{0} \\ \vdots & \vdots & \vdots & \vdots & \ddots & \vdots \\ \mathbf{G}_{N-1} & \mathbf{G}_{N-2} & \cdots & \cdots & \cdots & \mathbf{G}_0 \end{bmatrix},$$

$$\overline{\mathbf{G}}_j(q^{-1}) = \sum_{i=0}^{j-1}\mathbf{G}_i q^{-i}\,.$$

If all initial conditions are zero, the free response $\mathbf{f}$ is zero. If a unit step is applied to the first input at time t, that is, $\Delta\mathbf{u} = [\mathbf{I}\ \mathbf{0} \cdots \mathbf{0}]^T$, the expected output sequence $[\hat{\mathbf{y}}(t+1)^T\ \hat{\mathbf{y}}(t+2)^T \cdots \hat{\mathbf{y}}(t+N)^T]^T$ is equal to the first column of the matrix $\overline{\mathbf{G}}$. Thus, the first column of the matrix $\overline{\mathbf{G}}$ can be calculated as the step response of the plant when a unit step is applied to the first control signal.

The computation of the control input involves the inversion of an $nN \times nN$ matrix $\overline{\mathbf{G}}$ that requires a substantial amount of computation. If the control signal is kept constant after the first M control moves (that is, $\Delta\mathbf{u}(t+j-1) = \mathbf{0}_{m\times 1}$ for $j > M$), this leads to the inversion of an $nM \times nM$ matrix, which reduces the amount of computation. If so, the set of predictions affecting the cost function can be expressed as

$$\hat{\mathbf{y}} = \overline{\mathbf{G}}_s\Delta\mathbf{u}_s + \mathbf{f}\,, \tag{13}$$

where

$$\overline{\mathbf{G}}_s = \begin{bmatrix} \mathbf{G}_0 & \mathbf{0} & \cdots & \mathbf{0} \\ \mathbf{G}_1 & \mathbf{G}_0 & \cdots & \mathbf{0} \\ \vdots & \vdots & \ddots & \vdots \\ \mathbf{G}_{N-1} & \mathbf{G}_{N-2} & \cdots & \mathbf{G}_{N-M} \end{bmatrix},$$

$$\Delta\mathbf{u}_s = \begin{bmatrix} \Delta\mathbf{u}(t)^T & \Delta\mathbf{u}(t+1)^T & \cdots & \Delta\mathbf{u}(t+M-1)^T \end{bmatrix}^T.$$

The cost function can be rewritten as

$$J = \frac{1}{2}\left(\overline{\mathbf{G}}_s\Delta\mathbf{u}_s + \mathbf{f} - \mathbf{w}\right)^T \widetilde{\mathbf{Q}}\left(\overline{\mathbf{G}}_s\Delta\mathbf{u}_s + \mathbf{f} - \mathbf{w}\right) + \frac{1}{2}\Delta\mathbf{u}_s^T\widetilde{\mathbf{R}}\Delta\mathbf{u}_s, \tag{14}$$

where $\mathbf{w} = \begin{bmatrix}\mathbf{w}(t+1\,|\,t)^T & \mathbf{w}(t+2\,|\,t)^T & \cdots & \mathbf{w}(t+N\,|\,t)^T\end{bmatrix}^T$, $\widetilde{\mathbf{Q}} = diag(\mathbf{Q}, \cdots, \mathbf{Q})$ is a diagonal matrix, and $\widetilde{\mathbf{R}} = diag(\mathbf{R}, \cdots, \mathbf{R})$. Usually $\widetilde{\mathbf{Q}} = \mathbf{I}$ and $\widetilde{\mathbf{R}} = \mu \times \mathbf{I}$ are used and μ is called an input-weighting factor.

The optimal control input can be expressed as

$$\Delta\mathbf{u}_s = \left(\overline{\mathbf{G}}_s^T\widetilde{\mathbf{Q}}\overline{\mathbf{G}}_s + \widetilde{\mathbf{R}}\right)^{-1}\overline{\mathbf{G}}_s^T\widetilde{\mathbf{Q}}\left(\mathbf{w} - \mathbf{f}\right). \tag{15}$$

Because of the receding control strategy, only $\Delta\mathbf{u}(t)$ is needed at time step t. Thus, only the first m rows of the matrix $\left(\overline{\mathbf{G}}_s^T\widetilde{\mathbf{Q}}\overline{\mathbf{G}}_s + \widetilde{\mathbf{R}}\right)^{-1}\overline{\mathbf{G}}_s^T\widetilde{\mathbf{Q}}$ have to be computed.

To obtain the control input from Eq. (15), it is necessary to calculate matrix $\overline{\mathbf{G}}_s$ and vector $\mathbf{f}$. These matrix and vector values can be calculated recursively. From now on, the derivation will be described. By taking into account a new Diophantine equation corresponding to the prediction for $\hat{\mathbf{y}}(t+j+1\,|\,t)$, Eq. (5) can also be rewritten as follows:

$$\mathbf{I}_{n\times n} = \mathbf{E}_{j+1}(q^{-1})\mathbf{A}(q^{-1}) + q^{-(j+1)}\mathbf{F}_{j+1}(q^{-1}). \tag{16}$$

Subtracting Eq. (5) from Eq. (16) gives

$$\mathbf{0}_{n\times n} = \left[\mathbf{E}_{j+1}(q^{-1}) - \mathbf{E}_j(q^{-1})\right]\mathbf{A}(q^{-1}) + q^{-j}\left[q^{-1}\mathbf{F}_{j+1}(q^{-1}) - \mathbf{F}_j(q^{-1})\right]. \tag{17}$$

Because the matrix $\mathbf{E}_{j+1}(q^{-1}) - \mathbf{E}_j(q^{-1})$ is of order j, the matrix can be written as

$$\mathbf{E}_{j+1}(q^{-1}) - \mathbf{E}_j(q^{-1}) = \widetilde{\mathbf{P}}(q^{-1}) + \mathbf{P}_j q^{-j}, \tag{18}$$

where $\widetilde{\mathbf{P}}(q^{-1})$ is an $n\times n$ matrix polynomial of order smaller than or equal to $j-1$ and $\mathbf{P}_j$ is an $n\times n$ real matrix. By substituting Eq. (18) into Eq. (17)

$$\mathbf{0}_{n\times n} = \widetilde{\mathbf{P}}(q^{-1})\mathbf{A}(q^{-1}) + q^{-j}\left[\mathbf{P}_j\mathbf{A}(q^{-1}) + q^{-1}\mathbf{F}_{j+1}(q^{-1}) - \mathbf{F}_j(q^{-1})\right]. \tag{19}$$

Because $\mathbf{A}(q^{-1})$ is monic, it is easy to see that $\widetilde{\mathbf{P}}(q^{-1}) = \mathbf{0}_{n\times n}$. Therefore, from Eq. (18) the matrix $\mathbf{E}_{j+1}(q^{-1})$ can be calculated recursively by

$$\mathbf{E}_{j+1}(q^{-1}) = \mathbf{E}_j(q^{-1}) + \mathbf{P}_j q^{-j} \tag{20}$$

The following expressions can easily be obtained from Eq. (19):

$$\mathbf{P}_j = \mathbf{F}_{j,0} \tag{21}$$

$$\mathbf{F}_{j+1,i} = \mathbf{F}_{j,i+1} - \mathbf{P}_j\mathbf{A}_{i+1} \quad \text{for} \quad i = 0, \cdots, \delta(\mathbf{F}_{j+1}). \tag{22}$$

Also, it can easily be seen that the initial conditions for the recursion equation are given by

$$\mathbf{E}_1 = \mathbf{I}_{n\times n}, \tag{23}$$

$$\mathbf{F}_1 = q(\mathbf{I}_{n\times n} - \mathbf{A}) . \tag{24}$$

The free response vector $\mathbf{f}$ can be computed by the following recursive relationship:

$$\mathbf{f}_{j+1} = q\left(\mathbf{I} - \mathbf{A}(q^{-1})\right)\mathbf{f}_j + \mathbf{B}(q^{-1})\Delta\mathbf{u}(t+j) \text{, with } \mathbf{f}_0 = \mathbf{y}(t) \text{ and } \Delta\mathbf{u}(t+j) = \mathbf{0}_{m\times 1} \text{ for } j \geq 0 . \tag{25}$$

At every time instant, the receding horizon controller solves on-line an optimization problem by using Eqs. (15), (22), and (25) to compute optimal control inputs over a fixed number of future time instants, known as the time horizon.

3. Parameter Estimation

From Eq. (8) the optimal one-step-ahead prediction of $\mathbf{y}(t+1\,|\,t)$ is as follows:

$$\begin{aligned}\hat{\mathbf{y}}(t+1\,|\,t) &= \mathbf{F}_1(q^{-1})\mathbf{y}(t) + \mathbf{G}_1(q^{-1})\Delta\mathbf{u}(t) \\ &= -\hat{\mathbf{A}}_1\mathbf{y}(t) - \hat{\mathbf{A}}_2\mathbf{y}(t-1) - \cdots - \hat{\mathbf{A}}_{nA}\mathbf{y}(t-nA+1) + \hat{\mathbf{B}}_0\Delta\mathbf{u}(t) + \hat{\mathbf{B}}_1\Delta\mathbf{u}(t-1) + \cdots + \hat{\mathbf{B}}_{nB}\Delta\mathbf{u}(t-nB).\end{aligned} \tag{26}$$

Equation (26) can be expressed in the following inner product of the parameter vector $\hat{\boldsymbol{\theta}}(t)$ and the measurement vector $\boldsymbol{\varphi}(t)$:

$$\hat{\mathbf{y}}(t+1) = \hat{\boldsymbol{\theta}}^T(t)\cdot\boldsymbol{\varphi}(t) , \tag{27}$$

where

$$\hat{\boldsymbol{\theta}}^T(t) = \left[-\hat{\mathbf{A}}_1(t) \;\; -\hat{\mathbf{A}}_2(t) \;\; \cdots \;\; -\hat{\mathbf{A}}_{nA}(t) \;\; \hat{\mathbf{B}}_0(t) \;\; \hat{\mathbf{B}}_1(t) \;\; \cdots \;\; \hat{\mathbf{B}}_{nB}(t)\right] ,$$
$$\boldsymbol{\varphi}(t) = \left[\mathbf{y}(t)^T \;\; \mathbf{y}(t-1)^T \;\; \cdots \;\; \mathbf{y}(t-nA+1)^T \;\; \Delta\mathbf{u}(t)^T \;\; \Delta\mathbf{u}(t-1)^T \;\; \cdots \;\; \Delta\mathbf{u}(t-nB)^T\right]^T .$$

Equation (27) can be rewritten as

$$\hat{y}_i(t+1) = \hat{\boldsymbol{\theta}}_i^{\,T}(t)\cdot\boldsymbol{\varphi}(t) , \tag{28}$$

where $\hat{\boldsymbol{\theta}}_i$ denotes the i-th row of the matrix $\hat{\boldsymbol{\theta}}$.

The parameter vector $\hat{\boldsymbol{\theta}}_i(t)$ is estimated so that the following cost function is minimized:

$$J_i(t) = \sum_{j=0}^{t} \rho_{j/t}\left[y_i(j) - \hat{y}_i(j)\right]^2, \tag{29}$$

where

$$\rho_{t/t} = 1 ,$$
$$\rho_{j/t} = \lambda(t)\rho_{j/t-1}, \quad j = 1, 2, \cdots, t-1 .$$

Differentiating Eq. (29) with respect to $\hat{\boldsymbol{\theta}}_i(t)$ gives

$$\hat{\boldsymbol{\theta}}_i(t) = \hat{\boldsymbol{\theta}}_i(t-1) + \mathbf{F}_i(t)\boldsymbol{\varphi}(t-1)\left[y_i(t) - \hat{\boldsymbol{\theta}}_i^{\,T}(t-1)\cdot\boldsymbol{\varphi}(t-1)\right] , \tag{30}$$

$$\mathbf{F}_i(t) = \frac{1}{\lambda(t)}\left[\mathbf{F}_i(t-1) - \frac{\mathbf{F}_i(t-1)\boldsymbol{\varphi}(t-1)\boldsymbol{\varphi}^T(t-1)\mathbf{F}_i(t-1)}{\lambda(t) + \boldsymbol{\varphi}^T(t-1)\mathbf{F}_i(t-1)\boldsymbol{\varphi}(t-1)}\right], \tag{31}$$

where the covariance matrix $\mathbf{F}_i(0) > 0$ and $0 < \lambda(t) \leq 1$. The forgetting factor $\lambda(t)$ is calculated from the following equation [15]:

$$\lambda(t) = \lambda_0\lambda(t-1) + (1-\lambda_0) \quad \text{with} \quad \lambda_0 \leq 1 \text{ and } \lambda(0) \leq 1 \tag{32}$$

The parameters estimated by Eqs. (30) through (32) are used to design a generalized predictive controller. Figure 2 shows the schematic diagram of the generalized predictive controller combined with a parameter estimation algorithm.

4. AXIAL XENON OSCILLATION MODEL

An axial xenon oscillation model given in the literature [17,18] for a pressurized water reactor is used to examine the proposed control algorithm. The two-point model was derived from the nonlinear xenon and iodine balance equations and a one-group, one-dimensional, neutron diffusion equation with a nonlinear power reactivity feedback. In this model, the total power of the reactor core is assumed to be maintained constant even though the power density varies as a function of both time and position. In the axial xenon oscillation model, the following two-term spatial, harmonic-series solutions are assumed for the one-dimensional diffusion equation and the iodine and xenon balance equations, respectively:

$$\varphi(z,t) = \cos(\pi z / H) + P(t)\sin(2\pi z / H)\,, \tag{33}$$

$$x(z,t) = \cos(\pi z / H) + X(t)\sin(2\pi z / H)\,, \tag{34}$$

$$y(z,t) = \cos(\pi z / H) + Y(t)\sin(2\pi z / H)\,, \tag{35}$$

where $\varphi(z,t)$, $x(z,t)$, and $y(z,t)$ are the time-varying amplitudes of the flux and the xenon and iodine concentrations, respectively and the axial coordinate z is measured from the center of the cylinder that is of height H.

The spatial averages of the flux and the xenon and iodine concentrations for the lower half of a core are

$$\overline{\varphi}_1(t) = \frac{2}{\pi}[1 - P(t)]\,, \tag{36}$$

$$\overline{x}_1(t) = \frac{2}{\pi}[1 - X(t)]\,, \tag{37}$$

$$\overline{y}_1(t) = \frac{2}{\pi}[1 - Y(t)]\,. \tag{38}$$

The equations for the upper half of a core are

$$\overline{\psi}_2(t) = \frac{2}{\pi}[1 + P(t)]\,, \tag{39}$$

$$\overline{x}_2(t) = \frac{2}{\pi}[1 + X(t)]\,, \tag{40}$$

$$\overline{y}_2(t) = \frac{2}{\pi}[1 + Y(t)]\,. \tag{41}$$

An equation of the amplitude $P(t)$ is derived and solved by maintaining a reactor as nearly critical as possible using a variational estimate of the eigenvalues of the one-dimensional diffusion equation [17]:

$$-\beta_b P(t)^2 + 2(\beta_a - \beta_c)P(t) + \beta_b = 0\,, \tag{42}$$

where

$$\beta_a = \frac{1}{\Sigma_f}\left[4D\left(\frac{\pi}{H}\right)^2 + \frac{1}{2}(\Sigma_{a1} + \Sigma_{a2}) + \frac{32}{15\pi}(\sigma_X X_0 + 3\alpha_F \phi_0 \overline{\Sigma}_a)\right],$$

$$\beta_b = \frac{1}{\Sigma_f}\left[\frac{8}{3\pi}(-\Sigma_{a1} + \Sigma_{a2}) + \frac{64}{15\pi}\sigma_X X_0\right],$$

$$\beta_c = \frac{1}{\Sigma_f}\left[D\left(\frac{\pi}{H}\right)^2 + \frac{1}{2}(\Sigma_{a1} + \Sigma_{a2}) + \frac{8}{3\pi}(\sigma_X X_0 + \alpha_F \phi_0 \overline{\Sigma}_a)\right],$$

$$I_0 = \frac{\gamma_1 \Sigma_f \phi_0}{\lambda_I},$$
$$X_0 = \frac{(\gamma_1 + \gamma_X)\Sigma_f \phi_0}{\lambda_X + \frac{\pi}{4}\sigma_X \phi_0}.$$

The parameters in the preceding equations have their usual meanings, and ϕ_0, X_0, and I_0 are the time-independent steady-state values of the flux and the xenon and iodine concentrations, respectively. The dynamic equations of the other amplitude functions $X(t)$ and $Y(t)$ are obtained by integrating the iodine and xenon balance equations over the two regions of the core and substituting Eqs. (33) through (41):

$$\frac{dY(t)}{dt} = \left(\gamma_I \Sigma_f \frac{\phi_0}{I_0}\right) P(t) - \lambda_I Y(t), \tag{43}$$

$$\frac{dX(t)}{dt} = \left(\gamma_X \Sigma_f \frac{\phi_0}{X_0}\right) P(t) + \left(\lambda_I \frac{I_0}{X_0}\right) Y(t) - \lambda_X X(t) - \frac{2}{3}\sigma_X \phi_0 [P(t) + X(t)]. \tag{44}$$

The detailed axial xenon oscillation model is given in the literature [17,18].

The one-group diffusion parameters of the foregoing dynamic equations are listed in Table 1. The Σ_a is expressed as the combination of absorption cross sections of the fuel, moderator, structure, and control poison. To implement the proposed control algorithm, the partial-length rods can be selected as the control actuator so that the reactor power shape returns to its desired power shape.

Table 1. One-group diffusion parameters of the axial xenon oscillation model [17].

Parameter	Value
ϕ_0	2.1×10^{13} $[cm^{-2} \cdot s^{-1}]$
σ_X	2.6×10^{-18} $[cm^2]$
α_F	3.6×10^{-16} $[cm^2 \cdot s]$
γ_I	0.061
γ_X	0.003
λ_I	2.87×10^{-5} $[s^{-1}]$
λ_X	2.09×10^{-5} $[s^{-1}]$
D	0.375 $[cm]$
H	365.8 $[cm]$
Σ_f	0.65 $[cm^{-1}]$
$\nu\Sigma_f$	1.56 $[cm^{-1}]$
$\overline{\Sigma}_a$	1.523 $[cm^{-1}]$

5. APPLICATION TO THE AXIAL XENON OSCILLATION MODEL

Each region (half of a core) for the two-point xenon oscillation model has one input and one output, so the two-point xenon oscillation model has a total of two inputs and two outputs for the lower and upper halves of a core. Therefore, the control input is obtained from the first two rows of the following equation:

$$\Delta \mathbf{u}_s = \left(\overline{\mathbf{G}}_s^T \widetilde{\mathbf{Q}} \overline{\mathbf{G}}_s + \widetilde{\mathbf{R}}\right)^{-1} \overline{\mathbf{G}}_s^T \widetilde{\mathbf{Q}}(\mathbf{w} - \mathbf{f}), \tag{45}$$

where

$$\mathbf{w} = \left[w_1(t+1) \quad w_2(t+1) \quad w_1(t+2) \quad w_2(t+2) \quad \cdots \quad w_1(t+N) \quad w_2(t+N)\right]^T$$

= normalized target neutron flux,

$$\Delta \mathbf{u}_s = [\Delta u_1(t) \;\; \Delta u_2(t) \;\; \Delta u_1(t+1) \;\; \Delta u_2(t+1) \;\; \cdots \;\; \Delta u_1(t+M-1) \;\; \Delta u_2(t+M-1)]^T$$

$$= \begin{bmatrix} \Sigma_{a1}(t) - \Sigma_{a1}(t-1) \\ \Sigma_{a2}(t) - \Sigma_{a2}(t-1) \\ \vdots \\ \Sigma_{a1}(t+M-1) - \Sigma_{a1}(t+M-2) \\ \Sigma_{a2}(t+M-1) - \Sigma_{a2}(t+M-2) \end{bmatrix}$$

= variation in absorber cross sections Σ_{a1} and Σ_{a2} between two neighboring time steps,

subscripts '1' and '2' refer to the lower and upper halves of a core, respectively.

The orders of the matrix polynomials $\mathbf{A}(q^{-1})$ and $\mathbf{B}(q^{-1})$ are assumed to be 4 and 3, respectively. The initially adjusted parameters used in numerical simulations are the prediction horizon N, the control horizon M, and the output and input weighting matrices $\widetilde{\mathbf{Q}}$ and $\widetilde{\mathbf{R}}$. Generally, increasing the maximum prediction horizon N speeds up the step response of the closed loop system but induces an increase in overshoot, and the longer the prediction horizon, the less precise the prediction of the process output. Also, a longer prediction horizon increases the computational burden. Increasing the control horizon usually makes the system more active and hence allows a fast response to the system inputs. However, depending on the value of the control horizon, the closed-loop system response may become oscillatory with a large control horizon. The input-weighting factor μ plays an important role in determining the behavior of the closed-loop system. When the factor decreases, the system can be unstable. As the input-weighting factor increases, the response become well damped but is slowed down. Considering these facts, in all simulations the following parameters are used:

$$N = 10, \quad M = 1, \quad \widetilde{\mathbf{Q}} = \mathbf{I}, \text{ and } \widetilde{\mathbf{R}} = 10 \times \mathbf{I}.$$

Three different numerical simulations were performed to examine the proposed controller for three cases: (1) track the axial target shape, (2) remove the axial xenon oscillations induced by a perturbation, and (3) adapt to the parameters change. First, a numerical simulation was performed to observe the tracking performance of the proposed controller for the axial target flux shape that changes by step or ramp. Figure 3 shows its performance. The normalized target flux for upper half of a reactor core decreases by step at $t = 20h$ and increases linearly from $t = 70h$. The proposed controller tracks very well the target neutron flux change. Also, Figs. (c) and (d) show the parameter response estimated by the parameter estimation algorithm. These parameters updated at each time step are used to design the receding horizon controller.

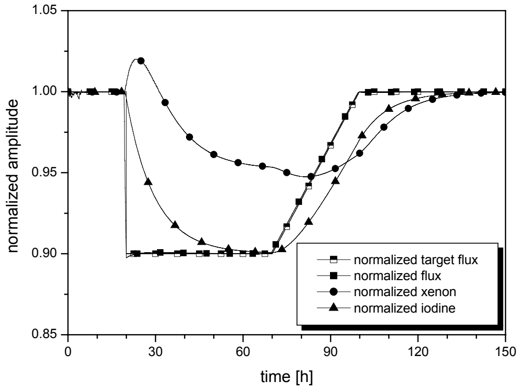

(a)

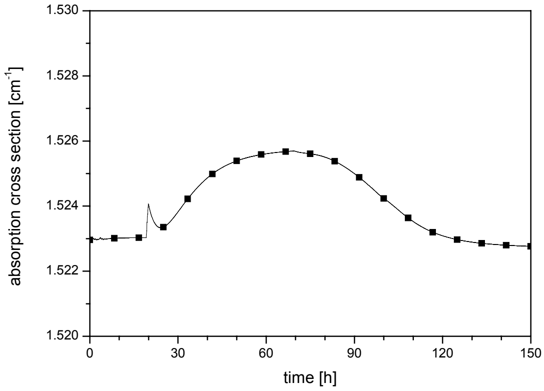

(b)

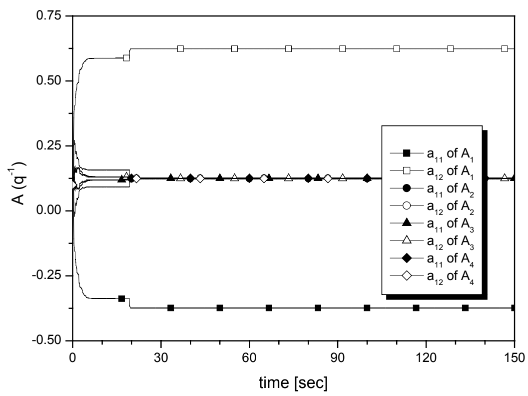

(c)

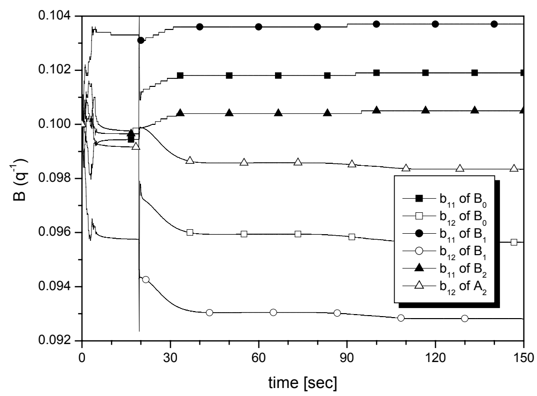

(d)

Figure. 3. Performance of the proposed controller due to ramp and step changes of axial target shape: (a) normalized target flux, flux, xenon, and iodine responses at the upper half of a reactor core; (b) macroscopic cross sections of the absorber in the upper half of a reactor core; (c) $\mathbf{A}(q^{-1})$ parameters; (d) $\mathbf{B}(q^{-1})$ parameters.

Figure 4 shows how well this controller removes the oscillations when xenon oscillations are induced externally. A perturbation is suddenly introduced at $t = 20h$ as shown in Fig. 4b and lasts for $2.5h$. Its amount is a 0.2% change of neutron absorber in the upper region. The free oscillations of the flux, xenon, and iodine are generated in case any control action is not taken for $67.5h$ after the introduction of the perturbation (refer to Fig. 4a). The proposed controller is activated at $t = 90h$ and removes the oscillations promptly. After that time, the normalized neutron flux tracks very well the axial target shape.

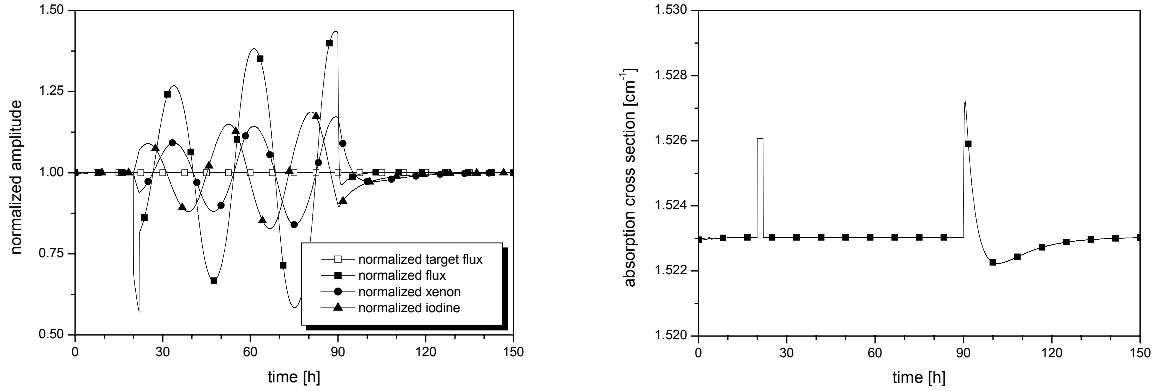

(a) (b)

Figure. 4. Performance of the proposed controller for the removal of free oscillations: (a) normalized target flux, flux, xenon, and iodine responses at the upper half of a reactor core; (b) macroscopic cross sections of the absorber in the upper half of a reactor core.

Figure 5 simulates the circumstances similar to Fig. 3. The difference is that a power reactivity coefficient α_F varies according to a ramp decrease and a step increase as a function of time (refer to Fig. 5c). The parameter value is less than that of the first simulation (refer to Table 1 and Fig. 3). The reactor usually becomes more unstable as the parameter decreases. But the performance for this case is similar to the results of the first numerical simulation.

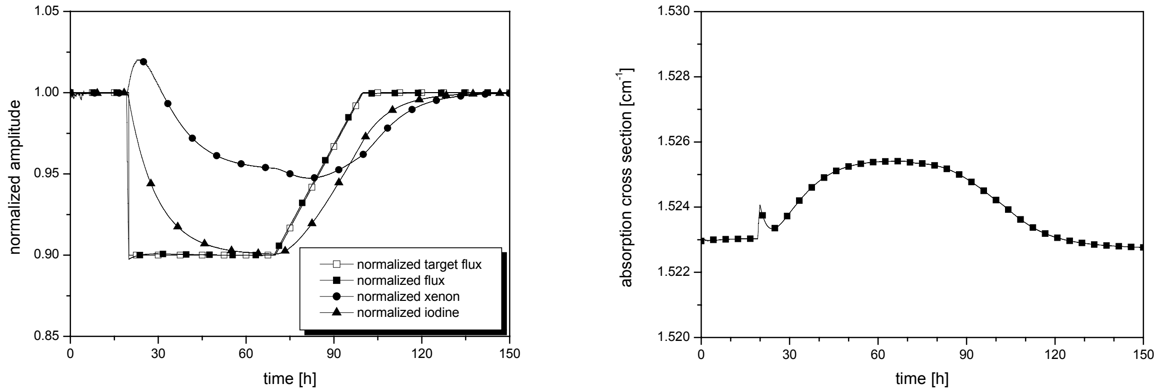

(a) (b)

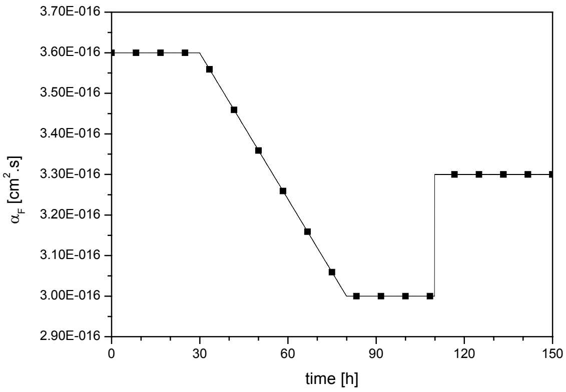

(c)

Figure 5. Performance of the proposed controller due to ramp and step changes of axial target shape (with parameter change): (a) normalized target flux, flux, xenon, and iodine responses at the upper half of a reactor core; (b) macroscopic cross sections of the absorber in the upper half of a reactor core; (c) change of the power reactivity coefficient in a reactor core.

6. CONCLUSIONS

A receding horizon control algorithm for the axial neutron flux shape control was presented. The concept of receding horizon control is to solve an optimization problem for a finite future at the current time and to implement the first optimal control input as the current control input. The procedure is then repeated at each subsequent instant. The reactor dynamics model used for computer simulations is a two-point xenon oscillation model based on the nonlinear xenon and iodine balance equations and a one-group, one-dimensional, neutron diffusion equation with nonlinear power reactivity feedback that adequately describes axial oscillations and treats the nonlinearities explicitly. The controlled process has two inputs and two outputs and is described by a matrix polynomial model. The reactor core is axially divided into two regions, and each region is assumed to have single input and single output and be coupled with the other region. In this model, the total power of the reactor core is assumed to be maintained constant even though the power density varies as a function of both time and position. The proposed control algorithm tracked very well the step and ramp changes of the axial target neutron flux shape without any residual flux oscillations between the upper and lower halves of a reactor core. Also, this controller showed good performance even under time-varying conditions and promptly removed oscillations induced by external means.

ACKNOWLEDGMENT

This work has been conducted under I-NERI Project supported by Korea Ministry of Science and Technology.

REFERENCES

1. M. Christie and C. G. Poncelet, "On the Control of Spatial Xenon Oscillations," Nucl. Sci. Eng., 51, 10 (1973).

2. S. H. Kim and J. Chang, "Exact Solution for Suboptimal Control of Nuclear Reactors with Distributed Parameters," Nucl. Sci. Eng., 78, 171 (1981).
3. N. Z. Cho and L. M. Grossman, "Optimal Control for Xenon Spatial Oscillations in Load Follow of a Nuclear Reactor," Nucl. Sci. Eng., 83, 136 (1983).
4. M. Winokur and L. Tepper, "Extension of Load Power Capability of a PWR Reactor by Optimal Control," IEEE Trans. Nucl. Sci., NS-31, 932 (1984).
5. M. H. Yoon and H. C. No, "Direct Numerical Technique of Mathematical Programming for Optimal Control of Xenon Oscillation in Load Following Operation," Nucl. Sci. Eng., 90, 203 (1985).
6. Lin and L. M. Grossman, "Optimal Control of a Boiling Water Reactor in Load-Following via Multilevel Methods," Nucl. Sci. Eng., 92, 531 (1986).
7. I.A. Gondal and R. A. Axford, "Optimal Xenon Control in Heterogeneous Reactor," IEEE Trans. Nucl. Sci., NS-33, 1722 (1986).
8. Gregory D. Wyss and Roy A. Axford, "Multidimensional Effects in Optimal Control Analysis for Nuclear Reactors," Nucl. Sci. Eng., 100, 458 (1988).
9. Y. H. Park and N. Z. Cho, "A Compensator Design Controlling Neutron Flux Distribution via Observer Theory," Ann. Nucl. Energy, 19, 513 (1992).
10. W. H. Kwon and A. E. Pearson, "A Modified Quadratic Cost Problem and Feedback Stabilization of a Linear System," IEEE Trans. Automatic Control, 22, 838 (1977).
11. J. Richalet, A. Rault, J. L. Testud, and J. Papon, "Model Predictive Heuristic Control: Applications to Industrial Processes," Automatica, 14, 413 (1978).
12. E. Garcia, D. M. Prett, and M. Morari, "Model Predictive Control: Theory and Practice – a Survey," Automatica, 25, 335 (1989).
13. M. V. Kothare, V. Balakrishnan, and M. Morari, "Robust Constrained Model Predictive Control Using Linear Matrix Inequality," Automatica, 32, 1361 (1996).
14. J. W. Lee, W. H. Kwon and J. H. Lee, "Receding Horizon H^{∞} Tracking Control for Time-Varying Discrete Linear Systems," Int. J. Control, 68, 385 (1997).
15. J. W. Lee, W. H. Kwon, and J. Choi, "On stability of Constrained Receding Horizon Control with Finite Terminal Weighting Matrix," Automatica, 34, 1607 (1998).
16. Eduardo F. Camacho and Carlos Bordons, Model Predictive Control, Springer-Verlag, London (1999).
17. R. J. Onega and R. A. Kisner, "An Axial Xenon Oscillation Model," Ann. Nucl. Energy, 5, 13 (1978).
18. Man Gyun Na, B. R. Upadhyaya, J. I. Choi, "Adaptive Control for Axial Power Distribution in Nuclear Reactors," Nucl. Sci. Eng., 129, 283, (1998).
19. Man Gyun Na, "Design of a Receding Horizon Control System for Nuclear Reactor Power Distribution," Nucl. Sci. Eng., Vol. 138, No. 3, pp. 305-314, July 2001.